International Journal of Nanomedicine

Dovepress
Taylor & Francis Group

Open Access Full Text Article

ORIGINAL RESEARCH

Solid Self-Microemulsifying Drug Delivery System for Improved Oral Bioavailability of Relugolix: Preparation and Evaluation

Zi-Lin Li[1]*, Guo-Xing Deng[1]*, Chuan-Zhou Fang[1]*, Yue-Qi Zhao[1], Jing Yuan[2], Liang Chen[3], Hai-Jun Zhong[1], Feng Guo[1]

[1]School of Pharmacy, Jiangxi Medical College, Nanchang University, Nanchang, 330006, People's Republic of China; [2]College of Basic Medicine and Forensic Medicine, Henan University of Science and Technology, Luoyang, 471000, People's Republic of China; [3]Jiangxi Prozin Pharmaceutical Co., LTD, Jian, 343100, People's Republic of China

*These authors contributed equally to this work

Correspondence: Feng Guo; Hai-JunZhong, School of Pharmacy, Jiangxi Medical College, Nanchang University, Nanchang, 330006, People's Republic of China, Tel +86 0791 86361839, Email fengguo@ncu.edu.cn; zhonghj@ncu.edu.cn

Purpose: To improve the oral absorption of relugolix (RLGL), which has low oral bioavailability due to its low solubility and being a substrate of P-glycoprotein (P-gp). A solid self-microemulsifying drug delivery system of relugolix (RLGL-S-SMEDDS) was prepared and evaluated in vitro and in vivo.

Methods: The composition of the solid self-microemulsifying drug delivery system (S-SMEDDS) was selected by solubility study and pseudo-ternary phase diagram, and further optimized by Design-Expert optimization design. The optimized RLGL-S-SMEDDS were evaluated in terms of particle size, zeta potential, morphology analysis, thermodynamic stability, drug release, flow properties, transporter pathways in Caco-2 cells, the influence of excipients on the intestinal transporters, transport within Caco-2 cell monolayers and transport in lymphocyte. In vivo pharmacokinetic study and toxicological study were also conducted.

Results: The optimum formulation for self-microemulsifying drug delivery system (SMEDDS) consists of Ethyl Oleate (26% of the weight), Solutol HS15 (49% of the weight), Transcutol HP (25% of the weight) and loaded relugolix (4.8 mg/g). The S-SMEDDS was then formed by adsorbing 2.4 g of SMEDDS onto 1 g of hydrophilic-200 silica. In phosphate buffered saline (PBS) (pH 6.8) release medium containing 1% tween 80, the vitro release studies showed 86% cumulative drug release for RLGL-S-SMEDDS and 3.6% cumulative drug release for RLGL suspensions. In vitro cellular uptake experiments revealed that the uptake of RLGL-S-SMEDDS by Caco-2 cells was three times higher than that of free RLGL, and that S-SMEDDS can enhance the drug absorption through lymphatic absorption and inhibition of intestinal transporter. In vivo pharmacokinetic evaluation demonstrated that the oral bioavailability of RLGL-S-SMEDDS was 1.9 times higher than that of RLGL-suspensions. There was no apparent cardiac, hepatic, splenic, pulmonary or renal toxicity on the surface discovered by pathological analysis after oral administration.

Conclusion: It is evident that S-SMEDDS may be a safe and effective method to improve oral absorption of drugs with low oral bioavailability.

Keywords: solid self-microemulsifying drug delivery system (S-SMEDDS), relugolix, microemulsion, oral bioavailability, P-glycoprotein

Introduction

According to the latest World Health Organization global cancer statistics for 2021, there were over 19.3 million new cancer cases worldwide and over 10 million cancer deaths.[1] In the world, prostate cancer is the most common cancer and the second leading cause of cancer deaths in men. According to statistics, about 10% of women at childbearing age suffer from endometriosis.[2] Leuprolide is the first-line drug for these diseases, but it has toxic side effects and low efficacy.[3] Relugolix (RLGL) is an orally active non-peptide gonadotropin-releasing hormone receptor antagonist used in the treatment of various sex hormone-related

Received: 23 September 2024
Accepted: 17 January 2025
Published: 25 January 2025

Graphical Abstract

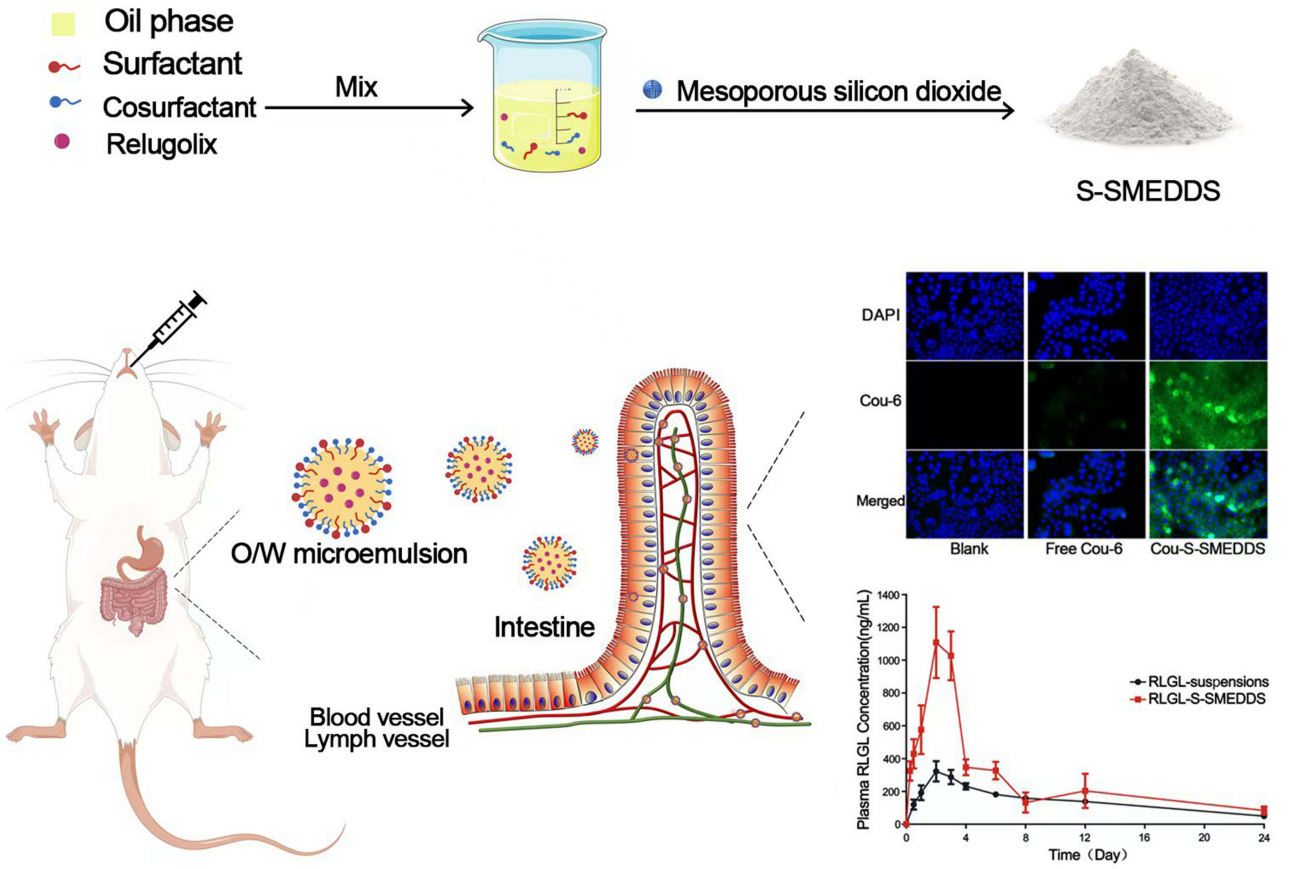

disorders.[4,5] Its chemical structure formula is shown in Figure 1A. RLGL has higher biosafety and efficacy than leuprolide, but its poor water solubility leads to low oral bioavailability.[6,7] A marketing application for Relugolix was submitted to the FDA in 2019 and approved in 2020. Since then, Relugolix has been marketed under the trade name Orgovyx. Relugolix may become the most important drug in the treatment of prostate cancer in the future due to its convenience, small side effects. However, its poor water solubility leads to only 12% oral bioavailability, and a drug delivery system is urgently needed to improve its oral bioavailability.

Self-microemulsifying drug delivery system (SMEDDS) has gained wide attention for its ability to improve the oral bioavailability of poorly water-soluble or lipophilic drugs. It is a homogeneous mixture containing oil, surfactant and co-surfactant that can spontaneously form a clarified system (particle size less than 100 nm) when dispersed in water.[8–10] The possible mechanisms by which self-microemulsion can promote oral absorption of drugs and improve their oral bioavailability are increased solubility and improved drug dissolution, the large amount of surfactants on the surface of self-microemulsions which increase the penetration into intestinal epithelial cells and promote the drug absorption, certain emulsifiers which can inhibit the efflux of drugs caused by P-glycoprotein, the lipid component of the prescription which can be degraded by pancreatic enzymes and biles to form smaller microemulsion droplets and bile salt micelles thereby increasing drug solubility and transmembrane transport efficiency and the lipid component of the oil phase which can also facilitate the absorption of drugs by lymphatically overcoming the first-pass effect of drugs and obstacles to the absorption of large molecules through the epithelial cells of the gastrointestinal tract.[11–15] The main reason that few self-emulsifying formulations are currently on the market is that all commercial liquid-based self-microemulsion products are encapsulated in hard gelatin capsules or soft gels, and the following disadvantages arise: the complexity of the production

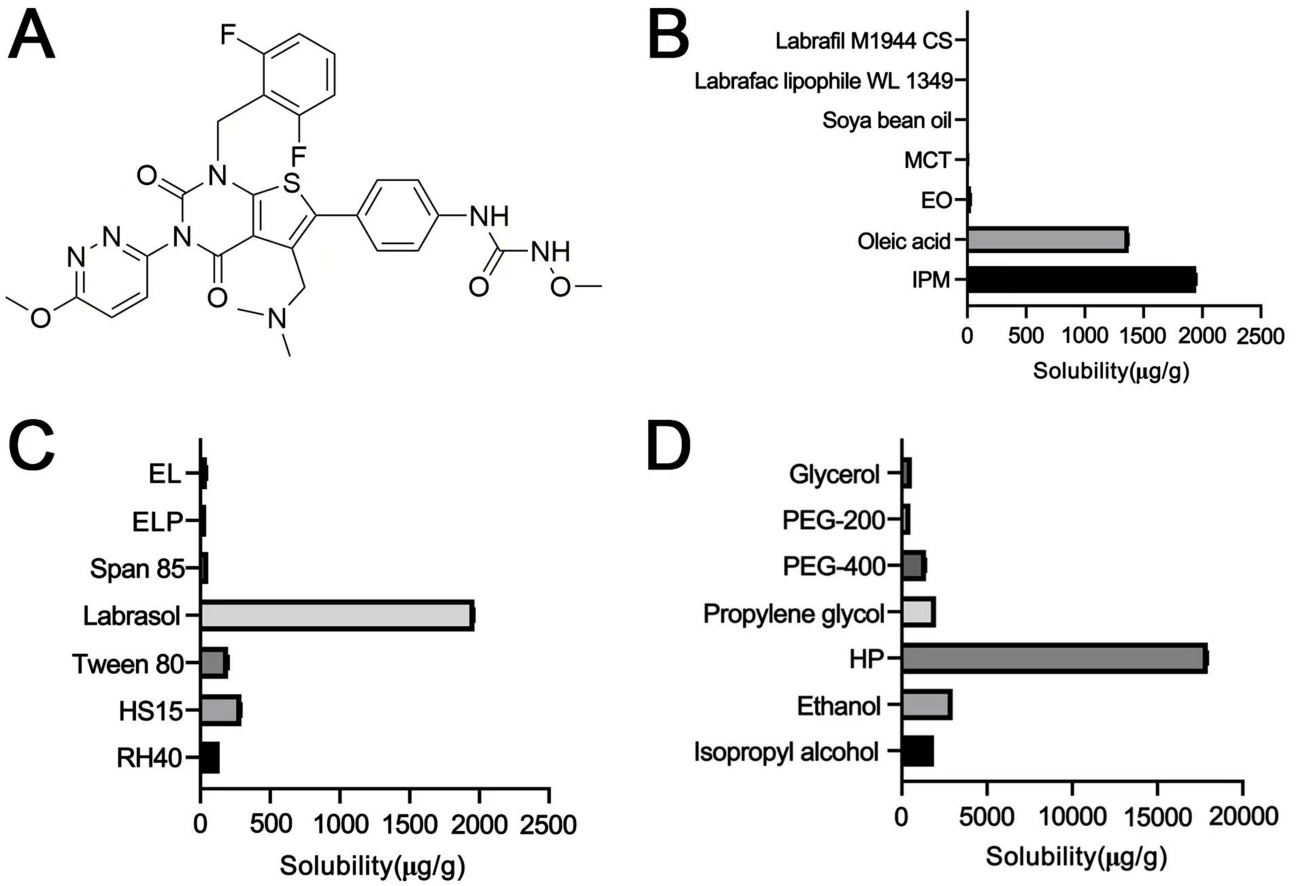

Figure 1 (**A**) Chemical structure of relugolix. Solubility of RLGL in various oils (**B**), surfactants (**C**) and co-surfactants (**D**). All values in μg/g, data are expressed as means ± SD (n=3).

process, resulting in high production costs, compatibility issues between formulation components and capsule shells and possible capsule leakage after long-term storage.[16–21]

The solid self-microemulsifying drug delivery system (S-SMEDDS) is a solid dosage form that combines the advantages of both self-emulsifying and solid formulations and overcomes the disadvantages of SMEDDS.[22,23] S-SMEDDS offer great advantages in terms of controlled drug release, prolonged gastric residence time and improved permeability, in addition to improving the absorption of poorly water-soluble drugs.[24–26] Moreover, S-SMEDDS can improve drug stability compared to SMEDDS.[27] As mentioned above S-SMEDDS may be an effective means to improve oral bioavailability of RLGL.

In this article, we report the preparation of a novel solid self-microemulsifying drug delivery system of RLGL (RLGL-S-SMEDDS) that is expected to have better therapeutic efficacy than RLGL-suspensions. To confirm our hypothesis, we prepared a self-microemulsion formulation for oral administration and performed detailed formulation optimization to select the appropriate excipients for oral administration. The morphology, particle size, zeta potential, thermodynamic and kinetic stability were examined. The solid carriers were screened for powder logical characterization. In vitro cellular uptake experiments, we established a Caco-2 cell monolayer model and a Caco-2 cell co-incubation model with lymphocytes to study the cellular uptake and transport of RLGL-S-SMEDDS. In vivo pharmacokinetic studies were carried out for determination of oral bioavailability of the drug. Histopathological analyses were made for preliminary evaluation of formulation safety.

Materials and Methods

Materials

Relugolix was from Takeda Pharmaceutical Industry Co., Ltd. (99%, Tokyo, Japan). Isopropyl myristate, ethanol, ethyl oleate, PEG 400 and Tween 80 were purchased from Aladdin Biochem Tech. Co., Ltd. (Shanghai, China). Transcutol HP (Gattefosse,

https://doi.org/10.2147/IJN.S497099

France), Solutol HS15 and Kolliphor P188 (BASF Ltd., Shanghai, China) were obtained as gift samples. Hydrophilic-200 silica and Sylysiak 320 were purchased from Yien Chemical Technology Co., Ltd. (Shanghai, China). Triton X-100, Dulbecco's modified Eagle's medium (DMEM), 3-(4,5-dimethylthiazol-2-yl)-2,5-diphenyltetrazolium bromide (MTT) and trypsin were purchased from Beijing Solarbio Sci&tech. Co., Ltd. (Beijing, China). Corning Matrigel Matrix were purchased from Corning Life Sciences (Wujiang) Co., Ltd. (Jiangsu, China). All the other chemicals and reagents were of analytical or HPLC grade and obtained from commercial sources.

Formulation and Optimization of RLGL-SMEDDS

Solubility Study

The solubility data of RLGL in various oils, surfactants and co-surfactants were determined by shake flask method. Excess RLGL was added into each tube containing the excipients (2 g), and the tubes were vortexed for 10 min and incubated at 25 °C for 48 h in THZ-82 digital water bath thermostat (Jiangsu Chenyang Electronics Co., Ltd. China) to reach equilibrium. The content of RLGL was measured by HPLC method.

Compatibility Test

To visually evaluate the self-emulsifying ability of a certain oil, surfactant and co-surfactant combination, a compatibility test was conducted according to the literature. Briefly, selected oils, surfactants and co-surfactants were mixed for 5 min in 4:4.5:1.5 (w/w) using a vortex mixer, and the above mixture was diluted by water to 20-fold its volume at 37 °C with gentle agitation.[28]

Construction of Pseudoternary Phase Diagram

Pseudoternary phase diagrams were constructed to obtain the concentration range of components for microemulsions.[29] The weight ratio of surfactant to co-surfactant (Km) was varied as 1:9, 2:8, 3:7, 4:6, 5:5, 6:4, 7:3, 8:2 and 9:1. For each pseudoternary phase diagram at a specific surfactant/co-surfactant weight ratio, the oily mixtures of oil, surfactant and co-surfactant were prepared with the weight ratio of oil to the mixture of surfactant and co-surfactant at 1:9, 2:8, 3:7, 4:6, 5:5, 6:4, 7:3, 8:2 and 9:1, respectively. Water was added drop by drop to each oily mixture under proper magnetic stirring at 37 °C until the mixture became clear at a certain point.[30] The concentrations of the components were recorded in order to complete the pseudoternary phase diagrams, and then the contents of oil, surfactant, co-surfactant and water at appropriate weight ratios were selected based on these results.

Experimental Design

The most appropriate ratio of K_m and oil was determined using central composite design (CCD). In this study, 13-run, two-factor, two-level CCD statistical screening design was used to optimize the formulation factors and the effects of Km and oil phase ratio on particle size and drug loading were investigated.[31,32] The statistical analysis was performed using Design-Expert® software (version 8.0.6.1).

Preparation of RLGL-SMEDDS

Ethyl Oleate (0.26 g), Solutol HS15 (0.49 g), Transcutol HP (0.25 g) and RLGL (4.8 mg) was successively placed in a clean vial, vortex ultrasonically mixed, and stirred in a 70 °C thermostatic water bath until the RLGL were completely dissolved. In the bottle, a clear and transparent RLGL-SMEDDS was obtained.

Characterization of RLGL-SMEDDS

Particle Size, Zeta Potential and Morphology

The samples were diluted with distilled water under gently stirring for 5 min and the particle size, polydispersity index (PDI), and zeta potential were measured by dynamic light scattering using a Brookhaven system (NanoBrook-173Plus, Brookhaven Instrument, USA).

The freshly prepared RLGL-SMEDDS sample was diluted 50-fold with distilled water, and an appropriate amount of the solution was dropped on a microporous copper mesh, dried naturally, stained with 2% phosphotungstic acid, and observed under a transmission electron microscope (TEM, H-600, Hitachi, Japan).

Effect of pH and Robustness to Dilution

In this paper, RLGL-SMEDDS was diluted 50-fold, 100-fold and 250-fold with distilled water, pH 1.2 and pH 6.8 buffers, respectively and left for 24 h. The phase transparency, drug precipitation and phase separation of the system were observed.

Cloud Point

The self-microemulsion was diluted with distilled water and stored in a water bath. The initial temperature of the water bath was 25 °C and was increased 5 °C every 10 min and the corresponding cloud point temperature was read visually at the first sign of turbidity.

Stability Studies

SMEDDS were subjected to different stress conditions including heating/cooling, freeze/thaw and centrifugation stresses. During this study, RLGL-SMEDDS was heated to 45 °C and held for 36 h, then cooled to 4 °C and held for 36 h, the formulation was subjected to three such hot and cold cycles. RLGL-SMEDDS was also kept at −20 °C for 36 h and then at 4 °C for 36 h, and the formulation underwent 3 such freeze/thaw cycles. In addition, centrifugal stress studies were performed with the preparation being under centrifugation at 5000 rpm for 30 min. After each stress study, the preparation was examined for phase separation and drug precipitation.

Formulation and Optimization of RLGL-S-SMEDDS

The S-SMEDDS was prepared by solid adsorption method, harnessing one of the water-soluble carriers (PEG 4000, PEG 6000, mannitol and lactose) or the water-insoluble carriers (Sylysiak 320 and Hydrophilic-200 silica).[33,34] The liquid was added drop by drop from the microemulsion to 1 g of adsorbent, ground well while adding. When the powder was slightly moist and each adsorbent material was saturated with adsorption, the amount of liquid self-microemulsion adsorbed was recorded as the maximum adsorption amount of that material. The particle size, PDI and in vitro drug release of different solid self-microemulsions were determined to screen for suitable solid adsorbent carriers.

Characterization of RLGL-S-SMEDDS

Particle Size, Zeta Potential

The samples were diluted with distilled water by gently stirring for 5 minutes, and centrifuged at 1000 rpm for 10 min. The particle size, polydispersity index, and zeta potential were measured by dynamic light scattering using a Brookhaven system (NanoBrook-173Plus, Brookhaven Instrument, USA).

Scanning Electron Microscopy

The morphologies of RLGL, Hydrophilic-200 silica and RLGL-S-SMEDDS were recorded by scanning electron microscope (SEM, Regulus 8100, Japan). Samples were fixed on a brass specimen club using a double-sided carbon conductive adhesive tape and the SEM images were observed at 15 kV accelerating voltage.

In vitro Release Study

The in vitro dissolution test of RLGL (2 mg) and S-SMEDDS (equivalent to 2 mg of drug) was carried out utilizing ZRS-6G basket tablet dissolution tester (Tianda, China). Experiments were carried out in 100 mL of 1% tween 80 dissolution medium at different pH (1.2, 6.8 and 7.4), 100 rpm and 37± 0.5 °C.1 mL was withdrawn from the dissolution medium at different predetermined time points and filtered through 0.22 μm organic filter membrane. The volume withdrawn was replaced with 1 mL of fresh dissolution solution to maintain a constant volume. The samples were suitably diluted and the drug content was determined by HPLC at 291 nm. All data were obtained in triplicate and expressed as a percentage of cumulative drug release.

Powder X-Ray Diffraction

Powder X-ray diffractograms of RLGL, Hydrophilic-200 silica, physical mixtures of RLGL and Hydrophilic-200 silica, and RLGL-S-SMEDDS were recorded using X-ray diffractometer (Bruker, D8 ADVANCE, Germany).The experiment

was conducted at room temperature using monochromatic Cu/K-alfa radiation (1.542 Å) and analyzed between 5 and 60° (2θ). The voltage and current used were 40 kV and 40 mA, respectively and the chart speed was 10 mm/sec (2θ).

Flow Properties

The flowability and compressibility of solid self-microemulsion powders were evaluated by measuring three indices: rest angle (θ), Hausner ratio (HR), and Karl index (CI).

A funnel was taken and fixed on a wire stand so that its tip was fixed at a specific height (h) and the mixed solid self-microemulsion sample was poured into the funnel so that the tip of the formed vertebral powder just touches the tip of the funnel and the radius (r) of the powder pile is recorded at this point. Calculate rest angle (θ), tanθ= h /r.

A certain amount of solid self-microemulsion powder sample was taken and put into a 20 mL measuring cylinder and tapped until the volume no longer changed. The volumes before and after tapping were recorded as V_{before} and V_{after} respectively. Calculate the Hausner ratio of the sample, $HR=V_{before}/V_{after}$.

The stack density (ρb) of the sample powder was calculated as ρb= mass of powder/ V_{before}, and the vibrational density (ρt) was calculated as ρt = mass of powder/ V_{after}. Based on the experimental measurement data, the Karl index (CI) was calculated as CI (%) = (ρt - ρb)/ ρt × 100%.

Cell Studies

Cell Culture

Caco-2 human colon carcinoma cells were obtained from the Cell Bank of the Chinese Academy of Sciences (Shanghai, China), while Raji cells were from Procell Life Science&Technology Co.,Ltd. (Wuhan, China). Cells were respectively cultured in Roswell Park Memorial Institute (RPMI) 1640 or Minimum Essential Medium (MEM) with 10% (v/v) Fetal Bovine Serum (FBS), 1% (v/v) penicillin (100 U/mL) and streptomycin (0.1 mg/mL) in 5% CO_2 atmosphere and 95% relative humidity at 37 °C.

Cytotoxicity

The cytotoxicity of Free RLGL, RLGL-SMEDDS and RLGL-S-SMEDDS on Caco-2 cells were investigated by MTT method.[35,36] Caco-2 cells were inoculated in 96-well plates at a cell density of 1×10^4 well^{-1} and incubated for 24 h allowing cells to adhere mutually. The cells were exposed to various preparations and incubated at various concentrations for 24 h, respectively. The absorbance value of each well was measured at a wavelength of 490 nm using a microplate reader.

Cellular Uptake

Coumarin 6 (COU) as a fluorescent marker used in cell experiments.[37,38] 4×10^5 Caco-2 cells were seeded in 6-well plates, incubated at 37 °C, 5% CO_2 for 24 h, then the old medium was discarded and the cells were washed twice with PBS. Serum medium diluted COU solution (Free COU) and COU-S-SMEDDS (COU final concentration of 300 ng mL^{-1}) were both seeded in three wells of the same plate and incubated at 37 °C for 2 h. After incubation, the supernatant was aspirated, and the Caco-2 cells were washed 3 times with pre-cooled PBS, trypsinized, centrifuged at 1500 rpm for 5 min, and washed twice with 1 mL PBS, redispersed into 500 μL PBS, and blowed evenly. 300 mesh cells were sieved into a flow tube, and the fluorescence intensity of COU was measured by flow cytometry, Ex/Em=488/530 nm, and no less than 10^4 cells were analyzed at each time.

Transporter Pathways in Caco-2 Cells

To investigate intestinal transporter pathways, Caco-2 cells were pretreated with efflux inhibitors, including verapamil (10 μg/mL), probenecid (0.2 mm) and elacridar (10 mm), at 37 °C for 1 h. Then, COU, COU-S-SMEDDS were mixed with efflux inhibitors and incubated with the cells for 3 h, respectively. After incubation, intracellular COU was detected by flow cytometry as described above.

The Effect of Excipients on the Intestinal Transporter

To investigate the effect of excipients on the intestinal transporter, Caco-2 cells were incubated with COU-EO, COU-Solutol HS15 and COU-Transcutol HP, respectively.[39,40] The concentration of the excipient is consistent with the prescription concentration and the final COU concentration was 300 ng/mL.

Transcellular Permeation Study

To establish an in vitro Caco-2 cell monolayer model, Caco-2 cells were placed in 12-well transwell plates with 0.4 μm pore polycarbonate film inserts (Corning, NY, USA).[41] For each transwell insert, 0.5 mL of cell culture medium containing 2×10^5 cells was added in the upper compartment and 1.5 mL of cell culture medium was added in the lower compartment. The medium of both compartments was changed every other day for the first 14 days and daily for the next 7 days. The integrity of Caco-2 cell monolayers was assessed by measuring transepithelial electrical resistance (TEER) and sodium fluorescein permeability. TEER was measured using a Millicell® ERS-2 voltameter (Bedford, MA, USA). After 21 days of incubation, cells with TEER values exceeding 500 Ω were selected for subsequent transport studies. After modeling, sodium fluorescein was added to the apical to test the membrane permeability.

$$\mathrm{TEER} = (\mathrm{TEER_T} - \mathrm{TEER_C}) \times \mathrm{A}$$

Where $\mathrm{TEER_T}$ is the measured TEER value of the Transwell chamber with cells (Ω); $\mathrm{TEER_C}$ is the measured TEER value of the Transwell chamber without cells (Ω); A is the area of the Transwell chamber ($\mathrm{cm^2}$).

To study transepithelial transport, 0.5 mL of free COU, COU-S-SMEDDS, COU-EO, COU-Solutol HS15 and COU-Transcutol HP were added to the apical side (AP) and 1.5 mL of PBS acceptor was added to the basal side (BP), similarly, 1.5 mL of these samples were added to the BP side and 0.5 mL of acceptor was added to the AP side. After 3 h, the COU content of the samples was measured by fluorescence spectrophotometer. The apparent permeability coefficient (P_{app}) of COU was calculated using the following equation:

$$P_{app} = (dQ/dt) \times (1/AC_0)$$

Where dQ/dt is the permeability rate (μg/s), C_0 is the initial concentration in the donor chamber (mg/mL), and A is the surface area of the filter ($\mathrm{cm^2}$), which was 1.12 $\mathrm{cm^2}$ in this study.

Transport in Lymphocyte

After normal culture of Caco-2 monolayer cells up to 15 days, Raji B cells at a density of 1×10^6 cells $\mathrm{well^{-1}}$ were added to the basal side of the transwell, and the culture medium on the apical side was changed daily, and that on the basal side was changed every half day.[15,42] The culture continued until the 21st day. Then 0.5 mL of free COU, COU-S-SMEDDS was added to the apical side and 1.5 mL of PBS acceptor was added to the basal side, similarly, 1.5 mL of these samples were added to the BP side and 0.5 mL of acceptor was added to the AP side. COU concentration was detected by method described above after 3 h of incubation at 37 °C.

Pharmacokinetic Study

To further understand the bioavailability of the formulation in vivo, experiments were conducted using Sprague-Dawley (SD) rats. SD rats were purchased from Hunan Slaughter Jingda Laboratory Animal Co., Ltd. (Hunan, China, No.430727220101126967). Female nude mice were placed in a pathogen-free environment with 5 mice per cage. The animals were acclimatized for 4–7 days before experimentation, fed with standard diet and allowed water ad libitum. All animal experiments were approved by the Ethics Committee of Nanchang University in accordance with the Guidelines for the Ethical Review of Laboratory Animal Welfare (GB/T 35892–2018) and ARRIVE 2.0.

Single oral administration: 12 female SD rats (250 ± 20 g) were randomly divided into 2 groups evenly, fasted for 12 h, free of drinking water, and underwent oral gavage of RLGL-suspension and RLGL-S-SMEDDS at a dose of 10.8 mg/kg, respectively. At 0.5, 1, 2, 3, 4, 6, 8, 12 and 24 h after administration, about 0.5 mL of blood was taken from the eyelids and placed in a heparinized EP tube, centrifuged at 10,000 rpm for 10 min, and the supernatant plasma was obtained. The drug concentration was determined by HPLC. DAS 3.0 pharmacokinetic software analysis.

Toxicological Study

After 7 days of PBS, S-SMEDDS, Solutol HS15 and Transcutol HP administration, the heart, liver, spleen, lung and kidney tissues of rats were dissected and fixed in 4% paraformaldehyde solution. The tissues were routinely taken, dehydrated, paraffin embedded, prepared to 4 μm thickness, HE stained, observed by light microscopy and photographed (microscope: Leica MD 1000, imaging system: Leica Application Suite). The pathology of each tissue was observed, photographed and analyzed.

HPLC Analysis

For the determination of RLGL solubility and in vitro drug release study, concentration of RLGL was determined by using HPLC. A 4.6×150 mm (3.5 μm particle size) Agilent Extend-C_{18} was used. The column temperature was maintained at 40 °C, while the flow rate was maintained at 0.7 mL/min. The mobile phase used water (0.05 mol/L monopotassium phosphate, pH=3) and acetonitrile (68:32[v/v]). Finally, the samples' concentrations were measured under ultraviolet detection at 291 nm.

Statistical Analysis

All the data are shown as means ± standard deviation (SD) and statistically evaluated using a one-way analysis of variance (ANOVA). $P < 0.05$ (*), $P < 0.01$ (**), $P < 0.001$ (***) and $P < 0.0001$ (****) were considered statistically significant.

Results and Discussion

Formulation and Optimization of RLGL-SMEDDS

Solubility Studies

Screening oil, surfactant and co-surfactant with maximum solubility potential is beneficial to optimum drug loading. The solubilities of RLGL in various oils, surfactants, and co-surfactants are shown in Figure 1B–D. Among the tested oils, the highest solubility of RLGL was detected in Isopropyl myristate (IPM), followed by Oleic acid and Ethyl Oleate (EO). Therefore, IPM, Oleic acid and EO were chosen as the oil phases for further studies. The three surfactants with the highest solubility for RLGL, namely, Labrasol, Solutol HS15 and Tween 80, were selected for further study. The co-surfactants were ordered as Transcutol HP, Ethanol and Propylene glycol.

Compatibility Tests

Compatibility testing is a key step in the design of formulations. Through the compatibility test, different oils, surfactants and co-surfactants possessing various emulsifying abilities can be compatible with each other in a mixture, which is beneficial to the optimization of the combination of oil, surfactant and co-surfactants.[43] By visual grading, IPM and Oleic acid as the oil phase could not form Grade "A" emulsion, indicating that IPM and Oleic acid were inferior in compatibility with surfactants and co-surfactants. When EO was combined with Tween 80 or Solutol HS15, Grade "A", "B" or "B~C" emulsion can be formed. The best compatibility was produced when Ethyl Oleate was mixed with Solutol HS15. The emulsifying effects of co-surfactants were all good, but ethanol and propylene glycol have certain toxicity and Transcutol HP has the maximum solubility to RLGL. EO is widely used in the food, cosmetics, and pharmaceutical industries with good safety.[44,45] According to reports (Gurjar et al, 2018), Solutol HS 15 has an inhibitory effect on p-gp, and Transcutol HP has the best effect on improving oral bioavailability of RLGL. The above compatibility results once again confirmed that it is a good choice to use EO as the oil phase, Solutol HS15 as the surfactant and Transcutol HP as the co-surfactant.

Construction of Phase Diagrams

As shown in Figure 2A, when Km was 1:9, 2:8, and 3:7, no clear and transparent microemulsion formed, suggesting that the emulsification effect of Transcutol HP was weaker than that of Solutol HS15. When the Km ratio was 9:1, the microemulsion was turbid. The area of microemulsion was smaller at 8:2, indicating that the single emulsifier was not effective. The area of microemulsion formed at Km 7:3 and 6:4 was the largest and equal. However, this range is still too

large. In order to obtain the appropriate Km when the amount of surfactant is as small as possible, CCD Experimental design was used to further determine the ratio of each component.

Experimental Design

CCD is the most frequently used method for response surface design. In this study, the oil content (X_1) and Km (X_2) were chosen as the two independent variables. A total of 13 experiments were conducted, and the response data for all experimental runs of CCD. The best-fit model was expressed in terms of coded factors as follows:

$$\text{Particle size} = 26.46 + 14.45X_1 - 2.86X_2 - 4.83X_1X_2 + 6.85X_1^2 - 0.77X_2^2$$

$$\text{Drug loading} = 4.89 - 1.14X_1 + 0.096X_2$$

ANOVA was used to validate the obtained models. It was shown that the p for both particle size and solubility regression equations were less than 0.01, implying a highly significant difference between the experimental models for this test. F was greater than 0.05, which was not significant, indicating that the quadratic term regression equation was a better fit, and that other factors interfered less with the model and the experimental error was relatively small.

As can be seen in Figure 2B, with the proportion of fixed oil phase in a certain range, the particle size increases slightly with the increase of Km, and the value of fixed Km increases with the increase of the proportion of oil phase. When the ratio of fixed oil phase was in a certain range, the drug loading increases slightly with the increase of Km while the value of fixed Km decreases with the increase of the ratio of oil phase. Overall, considering the side effects of a large number of surfactants and co-surfactants, the optimal formulations were as follows: Ethyl Oleate at 26% (w/w), Solutol HS15 at 49% (w/w), and Transcutol HP at 25% (w/w). The prediction error is less than 5%, indicating that the actual response is very close to the predicted value.

Characterization of RLGL-SMEDDS

In SMEDDS, the efficiency of self-emulsification can be assessed by measuring the emulsification rate and particle size distribution.[46] The latter is a key factor in determining the rate and extent of drug release and absorption. The particle size of RLGL-SMEDDS is 23.84 ± 0.43 nm (Figure 2C), PDI is less than 0.1, Zeta potential is −8.15 ± 3.63 mV, and self-emulsification time is less than 30s. Figure 2D shows the transmission electron microscope image of RLGL-SMEDDS. The results show that RLGL-SMEDDS is regular spherical or quasi-spherical with a size of about 25 nm, which is consistent with the particle size measurement of uniform distribution and good dispersion.[47–49]

After oral administration, SMEDDS is expected to gradually dilute upon contact with gastrointestinal fluids. Therefore, the stability of SMEDDS to dilution was monitored by diluting it 50, 100, and 250 times with distilled water as well as pH 1.2 and pH 6.8 buffers. It was observed that all the emulsions obtained were clarified and transparent without drug precipitation and phase separation, demonstrating their robustness to dilution. This also indicates the possibility of uniform release of the drug in vivo, in which case the formulation is expected to dilute gradually.

The cloud point is an important parameter for evaluating the stability of SMEDDS formulations.[50] The formulation is cloudy due to phase separation and drug precipitation, which can also hinder drug release. The cloud point temperature of the formulations was determined as in the range of 75–80 °C. This not only indicates a good thermal stability of the formulation but also gives an indication of unimpeded drug release.

Thermodynamic stability refers to the kinetic stability of the formulation, and the self-microemulsion should be able to tolerate various conditions in the gastrointestinal tract. The absence of precipitation and phase separation observed after heating/cooling, freeze/thaw and centrifugation stresses indicates good stability. The stability of RLGL-SMEDDS was good after 7 days at 4 °C. Precipitation was not observed, and particle size and PDI did not change significantly. This means that RLGL-SMEDDS can maintain good stability under these conditions.

Formulation and Optimization of RLGL-S-SMEDDS

Figure 3A shows the adsorption capacity of SMEDDS by different carriers, and that by water-soluble carriers is generally small. Then, the drug release in vitro was investigated. S-SMEDDS prepared by the water-soluble carrier could be completely released in water.

https://doi.org/10.2147/IJN.S497099

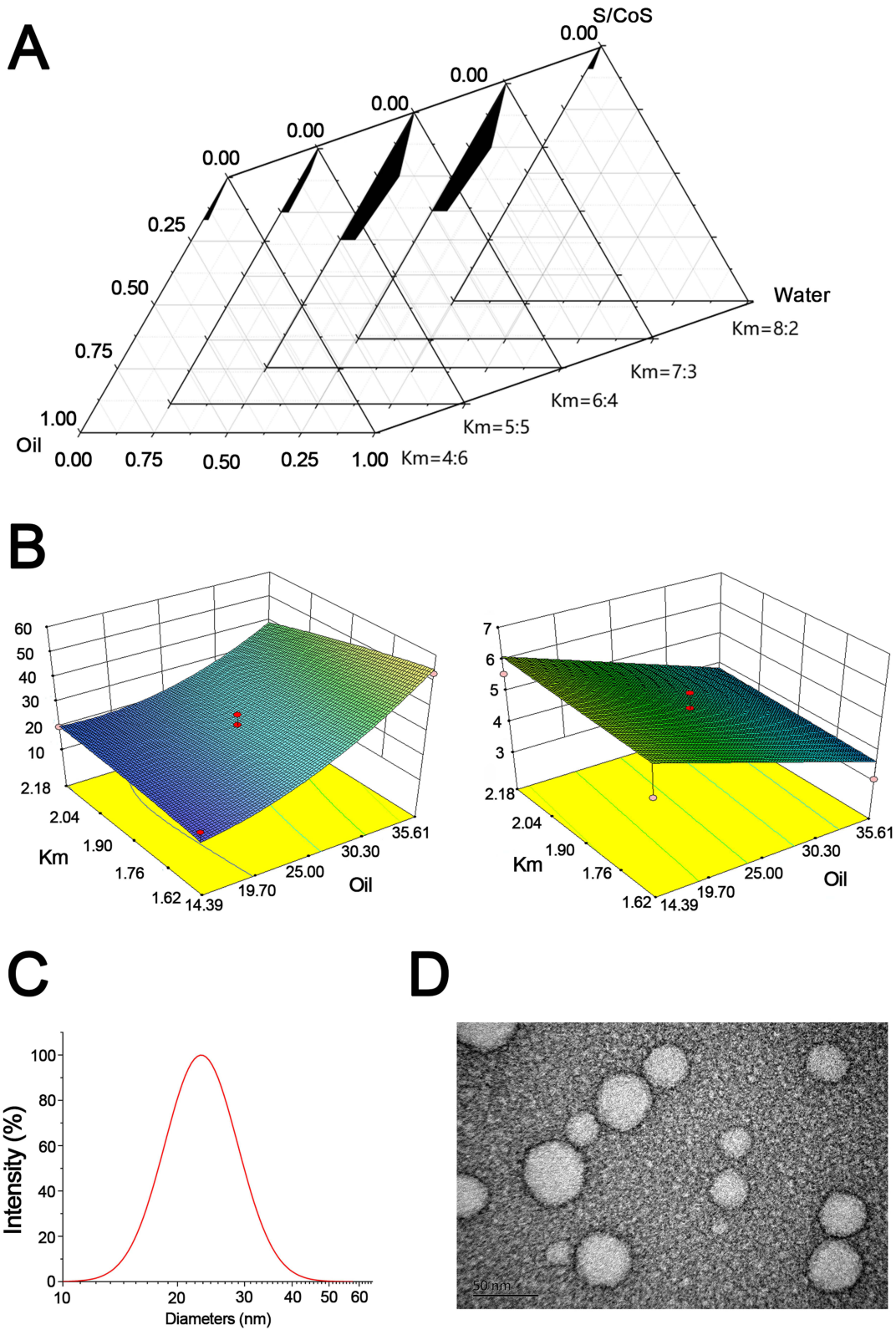

Figure 2 (**A**) Pseudoternary phase diagrams of the system composed of oil (Ethyl Oleate), surfactant (Solutol HS15), cosurfactant (Transcutol HP) and water. The black regions represent the regions of microemulsion (n=3). (**B**) Response surface plots (3D) showing the effect of oil (X_1) and Km (X_2) additions on particle size and drug loading. (**C**) Size distribution of RLGL-SMEDDS in water. (**D**) Transmission electron micrograph of RLGL-SMEDDS 50 nm.

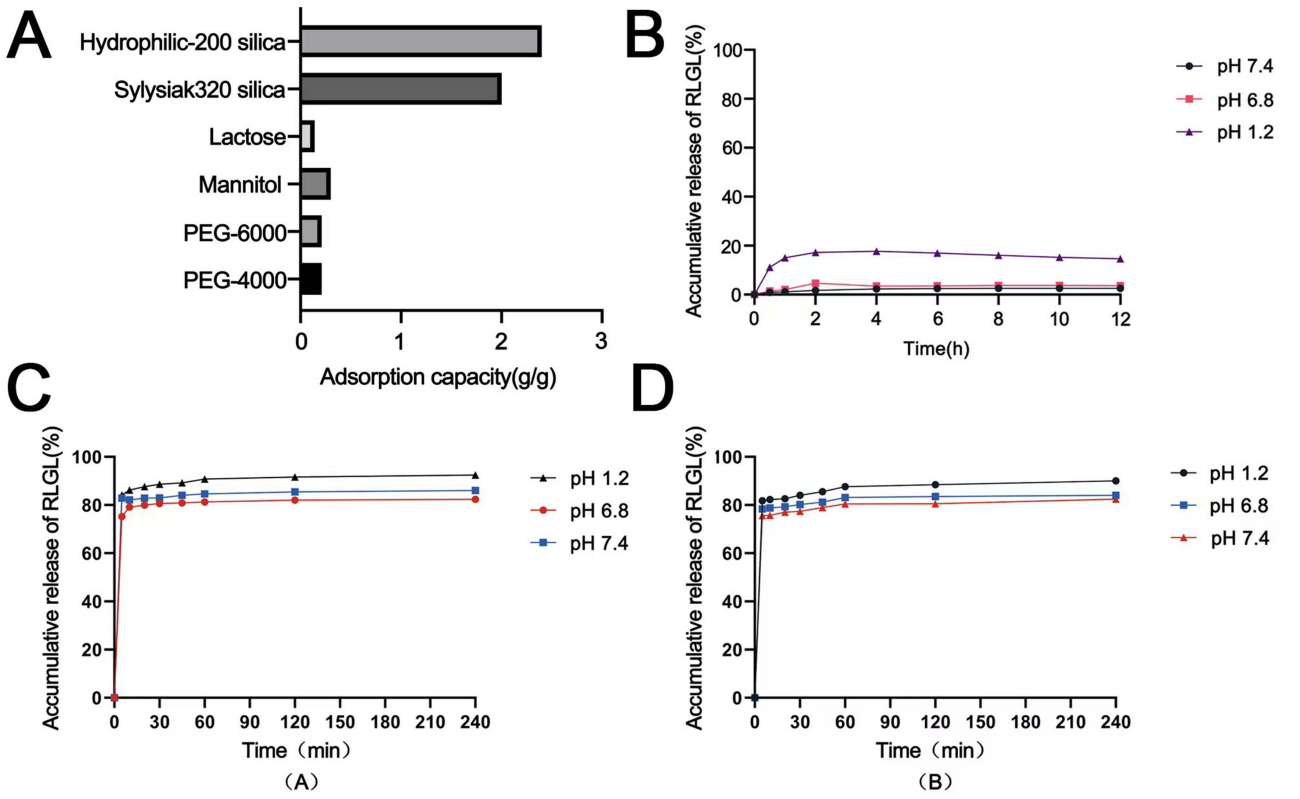

Figure 3 (**A**) Solid carrier adsorption capacity (n=3). (**B**) In vitro release of RLGL under different pH conditions (n=3). In vitro release of Hydrophilic-200 silica (**C**) and sylysiak 320 (**D**) under different pH conditions (n=3).

As shown in Figure 3B, the solubility of RLGL is pH dependent. 17% can be dissolved in 12 h at pH 1.2, while less than 5% can be dissolved in 12 h at pH 6.8 and pH 7.4. As shown in Figure 3C, the release of RLGL from solid formulations is significantly higher than that of RLGL. As for RLGL, there is a higher release of up to 90% at pH 1.2 for 5 min and 80% at pH 6.8 and 7.4 for 5 min. Solid self-microemulsion in contact with water results in rapid formation of O/W microemulsion. Because the drug is already dissolved in the mixture, the usual rate-limiting dissolution step required for crystallizing drugs is avoided.

As shown in Figure 3D, the two water-insoluble carriers released more than 80% within 5 minutes in different media. Therefore, two water-insoluble carriers with larger adsorption capacity were selected. After the two carriers were redispersed in water, it was discovered that the particle size was similar and the PDI was small. In conclusion, Hydrophilic-200 silica was selected as the solid adsorbent.

Characterization of RLGL-S-SMEDDS

Scanning electron microscopy showed the morphology of the various solid formulations (Figure 4A). The RLGL as an active pharmaceutical ingredient shows a crystalline structure, Hydrophilic-200 silica is a collection of particles with many pores on the surface. After being adsorbed, the pores on the surface of Hydrophilic-200 silica disappeared and no obvious RLGL bulk structure was observed, which indicated that the SMEDDS was adsorbed onto Hydrophilic-200 silica by the adsorption phenomenon.

As shown in Figure 4B, the high crystallinity of RLGL is reflected in the diffraction angles of 7.4°, 8.9°, 9.9°, 12.1°, 16.6° and 17.3°. These characteristic peaks are still observed in physical mixture and absent in S-SMEDDS, indicating that the physical state of RLGL is completely transformed from the crystalline to the amorphous state in the S-SMEDDS formulation.

https://doi.org/10.2147/IJN.S497099

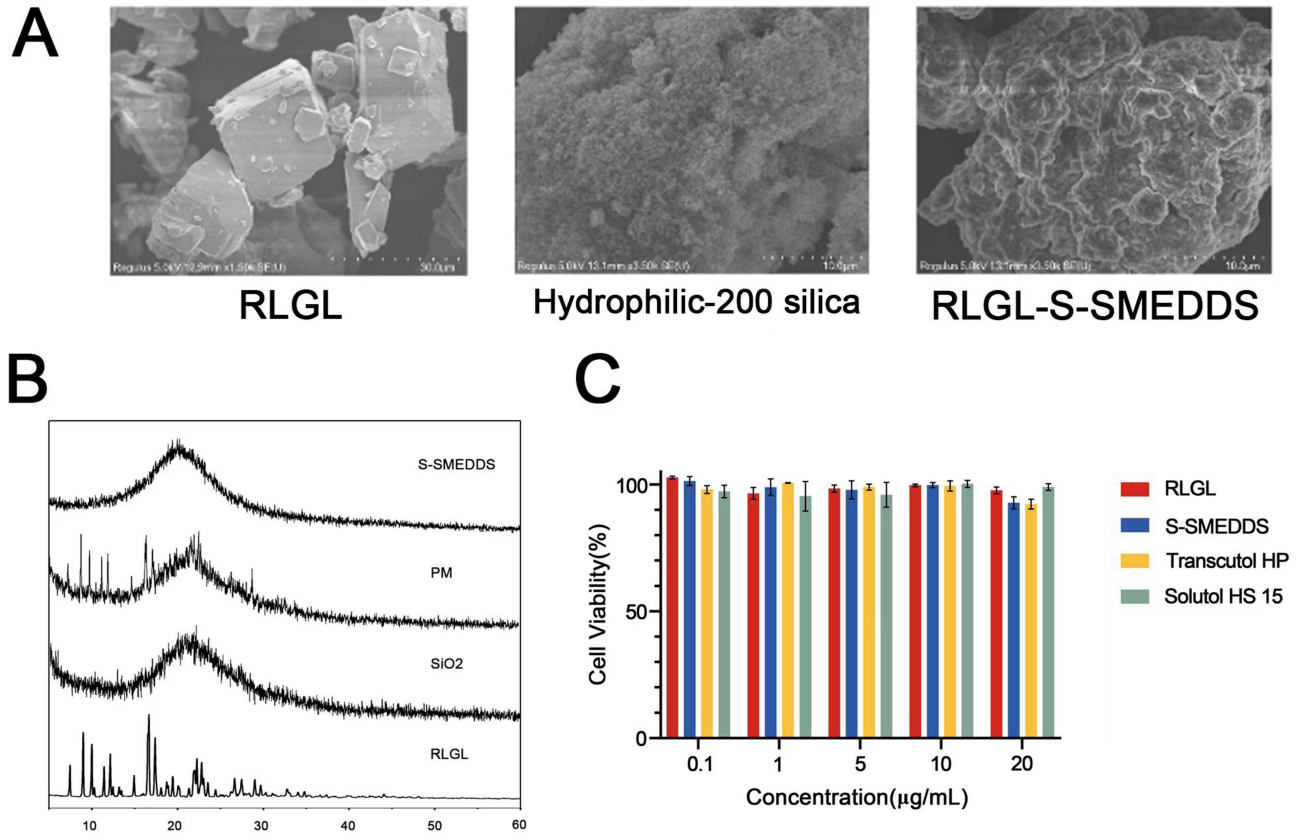

Figure 4 (**A**) Scanning electron micrographs of RLGL, Hydrophilic-200 silica and RLGL-S- SMEDDS. (**B**) Power X-ray diffraction of RLGL, Hydrophilic-200 silica, Physical mixture of RLGL and Hydrophilic-200 silica, and RLGL-S-SMEDDS. (**C**) Cell viabilities of Caco-2 cells after 24 h treatment with free RLGL, S-SMEDDS, Transcutol HP and Solutol HS15 at equivalent doses of RLGL (n=3).

S-SMEDDS has good flow characteristics, angle of repose (33.7°-34.2°), Hausner ratio (1.15–1.18), and compressibility (13.3–15.5%). From these results, it can be concluded that S-SMEDDS have good flow characteristics and compression properties, which contribute to the production of tablets with good cohesive properties and content uniformity.

Cytotoxic Studies

The Caco-2 cell monolayer model was chosen for this study. As an in vitro model, it is reliable and approved by the FDA and pharmaceutical companies for studying the cytotoxicity and behavior of developed agents drugs in the intestine. MTT results are shown in Figure 4C. RLGL, solid formulation and surfactant Transcutol HP, Solutol HS15 showed a better safety profile after 24 h incubation with Caco-2 cells within 0.1–20μg/mL concentrations (cell survival rate >90%). The excipients used in this prescription are relatively safe. They have been reported to be widely used in the food, cosmetic or pharmaceutical industries, which is consistent with the results of this experiment. Therefore, the present formulation has a good biosafety profile.

Cellular Uptake

The results of the flow cytometry experiment are shown in Figure 5A. The uptake of COU-S-SMEDDS is three times higher than that of free COU. This may be due to the rapid dispersion of the solid formulation in water to form O/W microemulsions with very small particle size, which penetrate the cell membrane more easily, and the surfactant in the prescription inhibits the efflux of P-gp and reduces the pumping of the drug. The exact mechanism needs to be further investigated.

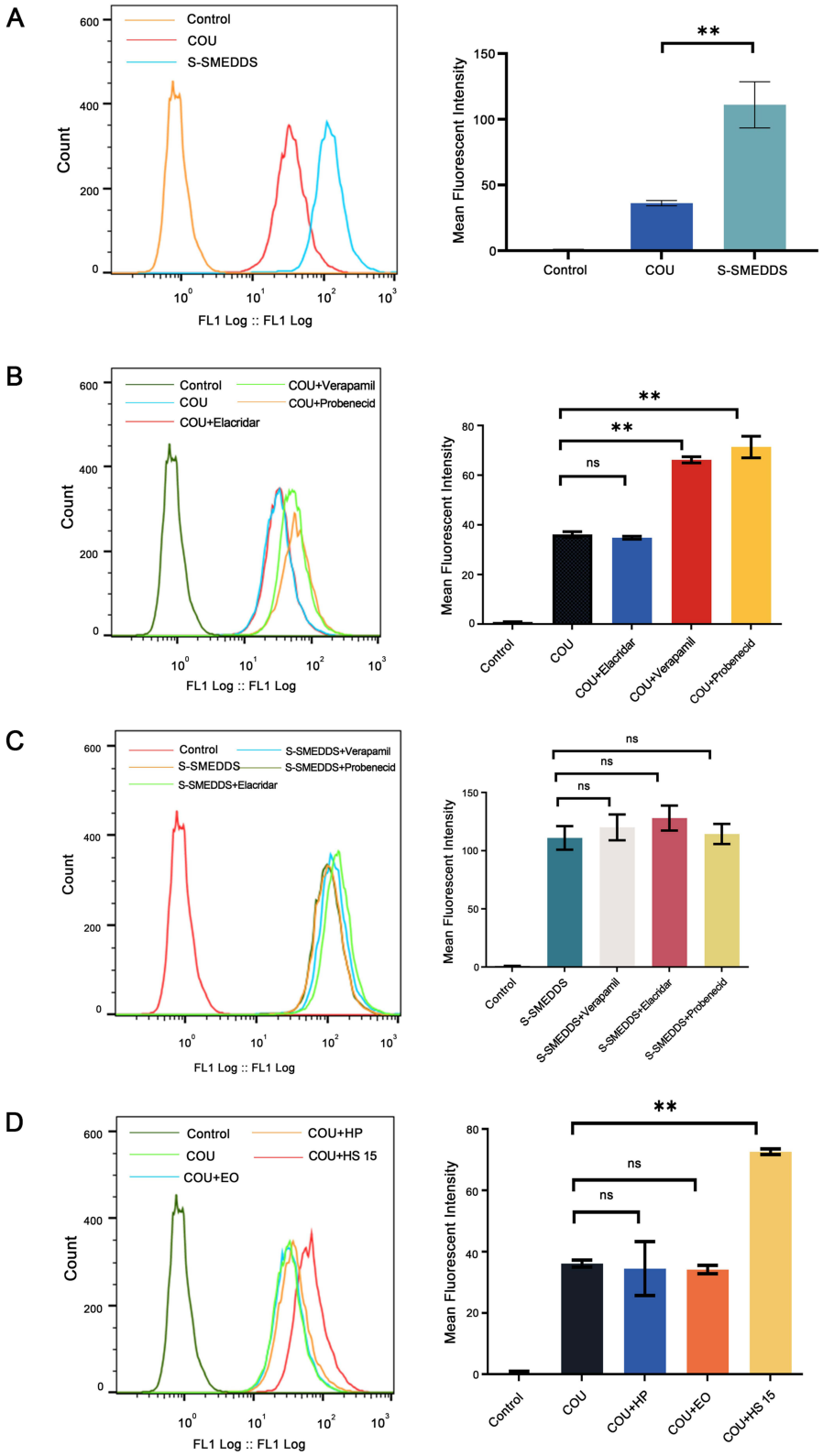

Figure 5 (**A**) Flow cytometric quantification of intracellular uptake of COU-S-SMEDDS and Free COU by Caco-2 cells after 3 h incubation at 37 °C (n=3). (**B**) Flow cytometric quantification of intracellular uptake of COU, COU+Elacridar, COU+Verapamil and COU+Probenecid in Caco-2 cells (n=3). (**C**) Flow cytometric quantification of intracellular uptake of S-SMEDDS, S-SMEDDS +Elacridar, S-SMEDDS+Verapamil and S-SMEDDS+Probenecid in Caco-2 cells (n=3). (**D**) Flow cytometric quantification of intracellular uptake of COU, COU + Ethyl Oleate, COU +Transcutol HP and COU+Solutol HS15 in Caco-2 cells (n=3). Statistical difference between groups: $p > 0.05$ ns and $p < 0.01$**.

https://doi.org/10.2147/IJN.S497099

Efflux Pathways in Caco-2 Cells

To better understand the mechanism of cellular efflux in drug, the specific efflux protein inhibitors verapamil, probenecid and elacridar were used to inhibit P-glycoprotein, multidrug resistance-associated protein 2 and breast cancer resistance protein, respectively. As shown in Figure 5C, the uptake of free COU pretreated with verapamil and probenecid was significantly higher than that of untreated free COU. The addition of verapamil and probenecid inhibited efflux proteins, confirming that the efflux of Caco-2 cells involves the P-gp and multidrug resistance-associated protein-2 pathways. Elacridar had no effect on cellular uptake.

The Effect of Excipients on the Intestinal Transporter

These were incubated S-SMEDDS with Caco-2 cells after pretreatment with three efflux protein inhibitors. The uptake results are shown in Figure 5B, with no significant difference between with and without efflux protein inhibitors. This result may be explained by that it is the surfactant that acts as an efflux protein inhibitor. We co-incubated the prescribed Ethyl Oleate, Transcutol HP and Solutol HS15 with COU, and the experimental results are shown in Figure 5D that no significant change in uptake was observed when COU was co-incubated with Transcutol HP and Ethyl Oleate, and a significant increase in uptake was observed when COU was co-incubated with Solutol HS 15. This suggests that Solutol HS 15 can effectively inhibit the intestinal transporter to increase drug uptake.

Transport Within Caco-2 Cell Monolayers

The cell monolayer with a resistance above 550 Ω was finally selected for the experiment by measuring the transmembrane resistance. As shown in Figure 6A, S-SMEDDS showed a significant increase in transport from AP-BP compared to free COU, along with a slight increase in transport from BP-AP. As shown in Figure 6B, free COU transport was increased after administration with Solutol HS 15 while no significant change was observed after co-administration with EO and Transcutol HP, which was due to the inhibition of intestinal transporter by Solutol HS15. However, the transport

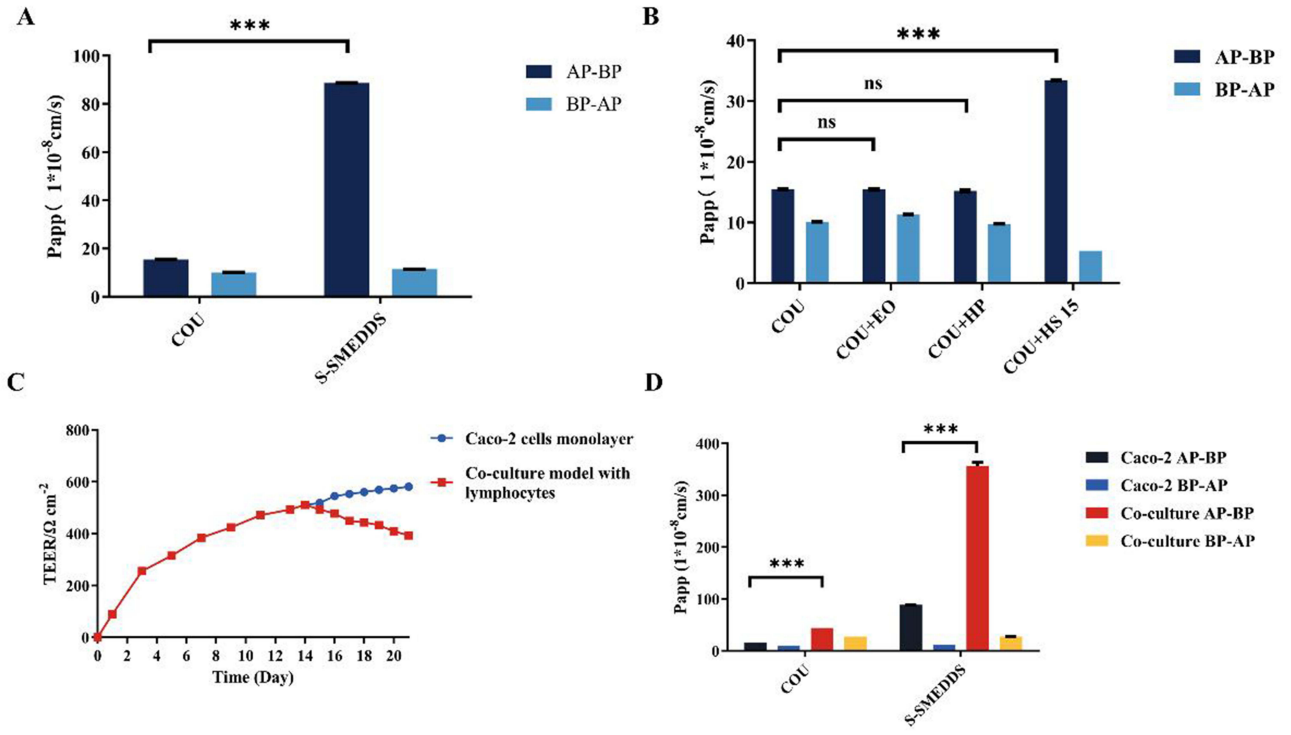

Figure 6 (**A**) the apparent permeability coefficient (Papp) of COU and S-SMEDDS. (**B**) the apparent permeability coefficient (Papp) of COU with Solutol HS15, Ethyl Oleate and Transcutol HP (n=3). (**C**) Transmembrane resistance for Caco-2 cell monolayer and co-culture model with lymphocytes for 21 days (n=3). (**D**) The apparent permeability coefficient (Papp) of COU and S-SMEDDS in Caco-2 cells monolayer and co-culture model with lymphocytes (n=3). Statistical difference between groups: $p > 0.05$ ns and $p < 0.001$***.

Table 1 Main Parameters of RLGL-Suspensions and RLGL-S-SMEDDS in vivo Pharmacokinetics (Mean ± SD, n=6)

Parameter	RLGL-Suspensions	RLGL-S-SMEDDS
C_{max} (μg/L)	371.299 ± 41.549	1192.807 ±2 34.301**
$AUC_{(0-t)}$ (μg/L·h)	3398.266 ± 118.780	6506.397 ± 2097.717*
$AUC_{(0-\infty)}$ (μg/L·h)	4035.504 ± 92.464	7691.996 ± 3244.116
$AUMC_{(0-t)}$ (μg/L·h)	29405.670 ± 766.057	46541.4 ± 24812.429
$AUMC_{(0-\infty)}$ (μg/L·h)	53046.117 ± 3106.867	105611.582 ± 90792.388
$MRT_{(0-t)}$ (h)	8.658 ± 0.275	6.789 ± 1.805
$MRT_{(0-\infty)}$ (h)	13.149 ± 0.826	12.054 ± 6.132
$T_{1/2}z$ (h)	8.960 ± 0.866	9.838 ± 6.259
T_{max} (h)	2.333 ± 0.577	2.333 ± 0.577

of free COU was less efficient than S-SMEDDS because the solid formulation formed an O/W microemulsion with water, and the small particle size further enhanced the transport. This is consistent with the results of our cellular uptake experiments.

Transport in Lymphocyte

The intestinal cells in the intestine are surrounded by the lamina propria and are connected to abundant capillaries and lymphatic vessels. Once the drug crosses the intestinal epithelium, it can be absorbed through the lymphatic vessels. Drugs transported through the intestinal lymphatic system enter the body's circulation without first passing through the liver which would enhance oral bioavailability. To investigate whether S-SMEDDS can be absorbed by lymphatic vessels, we established a Caco-2 cell monolayer co-cultured model with lymphocytes. As shown in Figure 6C, compared to the normal Caco-2 cell monolayer, the transmembrane resistance of co-culture model decreased after the addition of lymphocytes and eventually to 2/3 of that of the normal cell monolayer. This implies that the tightly connected cell monolayer was opened and the cell model was successfully established. As shown in Figure 6D, the apparent permeability coefficient of S-SMEDDS was significantly increased in the co-culture model, indicating that the preparation was available for uptake by lymphocytes.[51] There was also an increase in uptake from the BP-AP side because the tight cell monolayer was opened.

Pharmacokinetic Study

The main pharmacokinetic parameters of RLGL-suspension and RLGL-S-SMEDDS obtained by non-compartment mode are shown in Table 1 and Figure 7A. At the same RLGL dose, the maximum plasma concentration (Cmax) of the RLGL-

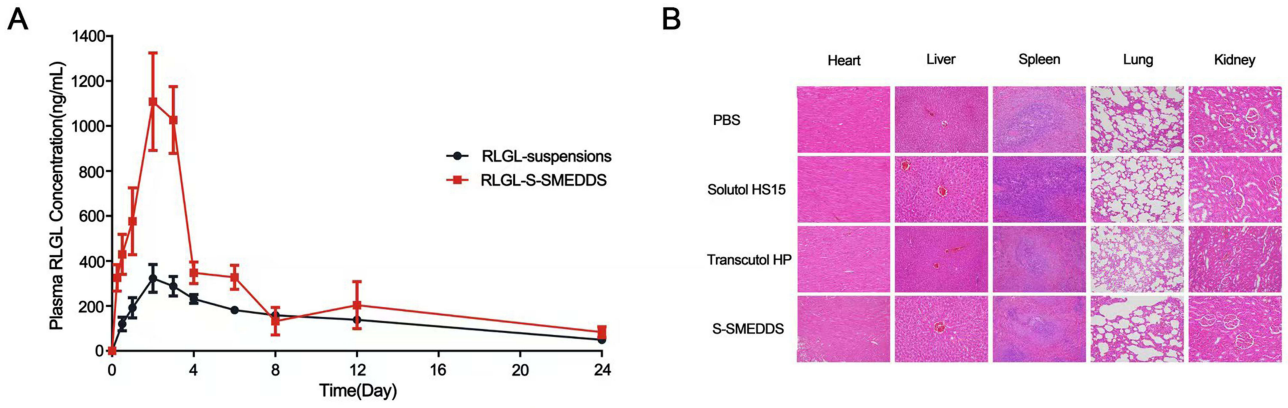

Figure 7 (**A**) Blood concentration-time profiles after oral administration of RLGL-S-SMEDDS and RLGL-suspensions (n=6). (**B**) Histological examination of heart, liver, spleen, lung and kidney tissues from animals treated with PBS, Solutol HS15, Transcutol HP and S-SMEDDS by hematoxylin and eosin (H&E) staining, scale bar 200 mm.

https://doi.org/10.2147/IJN.S497099

S-SMEDDS administration group was 3.2 times higher than that of RLGL suspension, and the area under the concentration-time curve ($AUC_{0-\infty}$) of the RLGL-S-SMEDDS administration group was 1.9 times higher than that of RLGL suspension, with no significant differences in other parameters. The reasons for the improved oral absorption and bioavailability of RLGL-S-SMEDDS may be the following: improved bioavailability through intestinal lymphatic transport avoiding the overtake effect, improved solubility of RLGL owing to S-SMEDDS, allowing drug remaining dissolved, the absorption-promoting effect of oil and surfactant, Solutol HS15 inhibiting intestinal transporter to improve absorption,58 and the small particle size of O/W-type microemulsion formed by S-SMEDDS avoiding phagocytosis by the reticuloendothelial system to prolong systemic circulation time.[52–59] Therefore, it can be concluded that S-SMEDDS can effectively improve the oral bioavailability of RLGL.

Toxicology Studies

The results of pathological examination on organs in each group are shown in Figure 7B. The results of all groups were similar to that of the PBS group, and no significant pathological changes were found in the heart, liver, spleen, lung and kidney. Based on the above findings, it can be confirmed that the surfactant has good biosafety at the administered dose and the solid self-microemulsion is non-toxic.

Conclusion

In the study, RLGL-S-SMEDDS was prepared and evaluated. It has uniform particle size distribution, good thermodynamic and kinetic stability and qualified powderological properties. The in vitro drug release for RLGL-S-SMEDDS was significantly enhanced compared to that for free RLGL. In vitro studies showed that the uptake of RLGL-S-SMEDDS by Caco-2 cells was three times higher than that of free RLGL by Caco-2 cells; in vivo studies indicated that RLGL-S-SMEDDS had a higher area under the drug-time curve than the RLGL-suspensions. The in vivo cytotoxicity assay and in vitro HE staining analysis showed that the various excipients have good biosafety and the solid self-microemulsions are non-toxic. In conclusion, the S-SMEDDS prepared in this study can improve oral bioavailability of RLGL and is biosafe, which is expected to provide a new idea and method for clinical application.

Abbreviations

RLGL, Relugolix; P-gp, P-glycoprotein; RLGL-S-SMEDDS, Solid self-microemulsifying drug delivery system of relugolix; SMEDDS, Self-microemulsifying drug delivery system; S-SMEDDS, Solid self-microemulsifying drug delivery system; PBS, Phosphate buffered solution; MTT, 3-(4,5-dimethylthiazol-2-yl)-2,5-diphenyltetrazolium bromide; CCD, Central composite design; PDI, Polydispersity index; COU, Coumarin 6; TEER, Transepithelial electrical resistance; AP, Apical side; BP, Basal side; Papp, Apparent permeability coefficient; IPM, Isopropyl myristate; EO, Ethyl Oleate; H&E, Hematoxylin & eosin.

Acknowledgment

This work was supported by the National Natural Science Foundation of China (Grant No. 32460240) and the Natural Science Foundation of Jiangxi Province, China (Grant No. 20202BAB206083).

Disclosure

The authors have no conflicts of interest to declare.

References

1. Siegel RL, Miller KD, Fuchs HE, et al. Cancer Statistics, 2021. *CA Cancer J Clin*. 2021;71(1):7–33. doi:10.3322/caac.21654
2. Shafrir AL, Farland LV, Shah DK, et al. Risk for and consequences of endometriosis: a critical epidemiologic review. *Best Pract Res Clin Obstet Gynaecol*. 2018;51:1–15. doi:10.1016/j.bpobgyn.2018.06.001
3. Huirne JAF, Lambalk CB. Gonadotropin-releasing-hormone-receptor antagonists. *Lancet*. 2001;358(9295):1793–1803. doi:10.1016/S0140-6736(01)06797-6
4. Osuga Y, Seki Y, Tanimoto M, et al. Relugolix, an oral gonadotropin-releasing hormone receptor antagonist, reduces endometriosis-associated pain in a dose-response manner: a randomized, double-blind, placebo-controlled study. *Fertil Steril*. 2021;115(2):397–405. doi:10.1016/j.fertnstert.2020.07.055

5. Saad F, Shore ND. Relugolix: a novel androgen deprivation therapy for management of patients with advanced prostate cancer. *Ther Adv Med Oncol*. 2021;13:1758835921998586. doi:10.1177/1758835921998586
6. Al-Hendy A, Lukes AS, Poindexter AN, et al. Treatment of uterine fibroid symptoms with relugolix combination therapy. *N Engl J Med*. 2021;384(7):630–642. doi:10.1056/NEJMoa2008283
7. Sahu KK, Tripathi N, Agarwal N, et al. Relugolix in the management of prostate cancer. *Expert Rev Anticancer Ther*. 2022;22(9):891–902. doi:10.1080/14737140.2022.2105209
8. Wu W, Wang Y, Que L. Enhanced bioavailability of silymarin by self-microemulsifying drug delivery system. *Eur J Pharm Biopharm*. 2006;63(3):288–294. doi:10.1016/j.ejpb.2005.12.005
9. Kang BK, Lee JS, Chon SK, et al. Development of self-microemulsifying drug delivery systems (SMEDDS) for oral bioavailability enhancement of simvastatin in beagle dogs. *Int J Pharm*. 2004;274(1–2):65–73. doi:10.1016/j.ijpharm.2003.12.028
10. Holm R. Examination of oral absorption and lymphatic transport of halofantrine in a triple-cannulated canine model after administration in self-microemulsifying drug delivery systems (SMEDDS) containing structured triglycerides. *Eur J Pharm Sci*. 2003;20(1):91–97. doi:10.1016/s0928-0987(03)00174-x
11. Gursoy RN, Benita S. Self-emulsifying drug delivery systems (SEDDS) for improved oral delivery of lipophilic drugs. *Biomed Pharmacother*. 2004;58(3):173–182. doi:10.1016/j.biopha.2004.02.001
12. Zhang HJ, Yao M, Morrison RA, et al. Commonly used surfactant, tween 80, improves absorption of P-glycoprotein substrate, digoxin, in rats. *Arch Pharm Res*. 2003;26(9):768–772. doi:10.1007/BF02976689
13. Moreau H, Bernadac A, Gargouri Y, et al. Immunocytolocalization of human gastric lipase in chief cells of the fundic mucosa. *Histochemistry*. 1989;91(5):419–423. doi:10.1007/BF00493829
14. Borovicka J, Schwizer W, Mettraux C, et al. Regulation of gastric and pancreatic lipase secretion by CCK and cholinergic mechanisms in humans. *Am J Physiol*. 1997;273(2 Pt 1):G374–380. doi:10.1152/ajpgi.1997.273.2.G374
15. Ye J, Gao Y, Ji M, et al. Oral SMEDDS promotes lymphatic transport and mesenteric lymph nodes target of chlorogenic acid for effective T-cell antitumor immunity. *J Immunother Cancer*. 2021;9(7):e002753. doi:10.1136/jitc-2021-002753
16. Mandic J, Zvonar Pobirk A, Vrecer F, et al. Overview of solidification techniques for self-emulsifying drug delivery systems from industrial perspective. *Int J Pharm*. 2017;533(2):335–345. doi:10.1016/j.ijpharm.2017.05.036
17. Park H, Ha ES, Kim MS. Current status of supersaturable self-emulsifying drug delivery systems. *Pharmaceutics*. 2020;12(4):365. doi:10.3390/pharmaceutics12040365
18. Newton M, Petersson J, Podczeck F, et al. The influence of formulation variables on the properties of pellets containing a self-emulsifying mixture. *J Pharm Sci*. 2001;90(8):987–995. doi:10.1002/jps.105
19. Tuleu C, Newton M, Rose J, et al. Comparative bioavailability study in dogs of a self-emulsifying formulation of progesterone presented in a pellet and liquid form compared with an aqueous suspension of progesterone. *J Pharm Sci*. 2004;93(6):1495–1502. doi:10.1002/jps.20068
20. Abdalla A, Mader K. Preparation and characterization of a self-emulsifying pellet formulation. *Eur J Pharm Biopharm*. 2007;66(2):220–226. doi:10.1016/j.ejpb.2006.11.015
21. Franceschinis E, Voinovich D, Grassi M, et al. Self-emulsifying pellets prepared by wet granulation in high-shear mixer: influence of formulation variables and preliminary study on the in vitro absorption. *Int J Pharm*. 2005;291(1–2):87–97. doi:10.1016/j.ijpharm.2004.07.046
22. Nazzal S, Khan MA. Controlled release of a self-emulsifying formulation from a tablet dosage form: stability assessment and optimization of some processing parameters. *Int J Pharm*. 2006;315(1–2):110–121. doi:10.1016/j.ijpharm.2006.02.019
23. Almeida SRD, Tippavajhala VK. A rundown through various methods used in the formulation of solid self-emulsifying drug delivery systems (S-SEDDS). *AAPS Pharm Sci Tech*. 2019;20(8):323. doi:10.1208/s12249-019-1550-5
24. Setthacheewakul S, Kedjinda W, Maneenuan D, et al. Controlled release of oral tetrahydrocurcumin from a novel self-emulsifying floating drug delivery system (SEFDDS). *AAPS Pharm Sci Tech*. 2011;12(1):152–164. doi:10.1208/s12249-010-9568-8
25. Sermkaew N, Wiwattanawongsa K, Ketjinda W, et al. Development, characterization and permeability assessment based on caco-2 monolayers of self-microemulsifying floating tablets of tetrahydrocurcumin. *AAPS Pharm Sci Tech*. 2013;14(1):321–331. doi:10.1208/s12249-012-9912-2
26. Joyce P, Dening TJ, Meola TR, et al. Solidification to improve the biopharmaceutical performance of SEDDS: opportunities and challenges. *Adv Drug Deliv Rev*. 2019;142:102–117. doi:10.1016/j.addr.2018.11.006
27. Chityala PK, Khouryieh H, Williams K, et al. Effect of xanthan/enzyme-modified guar gum mixtures on the stability of whey protein isolate stabilized fish oil-in-water emulsions. *Food Chem*. 2016;212:332–340. doi:10.1016/j.foodchem.2016.05.187
28. Kawakami K, Yoshikawa T, Moroto Y, et al. Microemulsion formulation for enhanced absorption of poorly soluble drugs. I. Prescription design. *J Control Release*. 2002;81(1–2):65–74. doi:10.1016/s0168-3659(02)00049-4
29. Dixit AR, Rajput SJ, Patel SG. Preparation and bioavailability assessment of SMEDDS containing valsartan. *AAPS Pharm Sci Tech*. 2010;11(1):314–321. doi:10.1208/s12249-010-9385-0
30. Patel MH, Mundada VP, Sawant KK. Novel drug delivery approach via self-microemulsifying drug delivery system for enhancing oral bioavailability of asenapine maleate: optimization, characterization, cell uptake, and in vivo pharmacokinetic studies. *AAPS Pharm Sci Tech*. 2019;20(2):44. doi:10.1208/s12249-018-1212-z
31. Na YG, Huh HW, Kim MK, et al. Development and evaluation of a film-forming system hybridized with econazole-loaded nanostructured lipid carriers for enhanced antifungal activity against dermatophytes. *Acta Biomater*. 2020;101:507–518. doi:10.1016/j.actbio.2019.10.024
32. Son HY, Chae BR, Choi JY, et al. Optimization of self-microemulsifying drug delivery system for phospholipid complex of telmisartan using D-optimal mixture design. *PLoS One*. 2018;13(12):e0208339. doi:10.1371/journal.pone.0208339
33. Tan A, Rao S, Prestidge CA. Transforming lipid-based oral drug delivery systems into solid dosage forms: an overview of solid carriers, physicochemical properties, and biopharmaceutical performance. *Pharm Res*. 2013;30(12):2993–3017. doi:10.1007/s11095-013-1107-3
34. Jannin V, Musakhanian J, Marchaud D. Approaches for the development of solid and semi-solid lipid-based formulations. *Adv Drug Deliv Rev*. 2008;60(6):734–746. doi:10.1016/j.addr.2007.09.006
35. Berridge MV, Herst PM, Tan AS. Tetrazolium dyes as tools in cell biology: new insights into their cellular reduction. *Biotechnol Annu Rev*. 2005;11:127–152. doi:10.1016/S1387-2656(05)11004-7
36. Li W, Zhou J, Xu Y. Study of the in vitro cytotoxicity testing of medical devices. *Biomed Rep*. 2015;3(5):617–620. doi:10.3892/br.2015.481

37. Liu S, Cao Y, Ma L, et al. Oral antimicrobial peptide-EGCG nanomedicines for synergistic treatment of ulcerative colitis. *J Control Release*. 2022;347:544–560. doi:10.1016/j.jconrel.2022.05.025
38. Katila N, Duwa R, Bhurtel S, et al. Enhancement of blood-brain barrier penetration and the neuroprotective effect of resveratrol. *J Control Release*. 2022;346:1–19. doi:10.1016/j.jconrel.2022.04.003
39. Rahman MA, Hussain A, Hussain MS, et al. Role of excipients in successful development of self-emulsifying/microemulsifying drug delivery system (SEDDS/SMEDDS). *Drug Dev Ind Pharm*. 2013;39(1):1–19. doi:10.3109/03639045.2012.660949
40. Kollipara S, Gandhi RK. Pharmacokinetic aspects and in vitro-in vivo correlation potential for lipid-based formulations. *Acta Pharm Sin B*. 2014;4 (5):333–349. doi:10.1016/j.apsb.2014.09.001
41. Hubatsch I, Ragnarsson EG, Artursson P. Determination of drug permeability and prediction of drug absorption in Caco-2 monolayers. *Nat Protoc*. 2007;2(9):2111–2119. doi:10.1038/nprot.2007.303
42. Beloqui A, Brayden DJ, Artursson P, et al. A human intestinal M-cell-like model for investigating particle, antigen and microorganism translocation. *Nat Protoc*. 2017;12(7):1387–1399. doi:10.1038/nprot.2017.041
43. Chen Y, Li G, Wu X, et al. Self-microemulsifying drug delivery system (SMEDDS) of vinpocetine: formulation development and in vivo assessment. *Biol Pharm Bull*. 2008;31(1):118–125. doi:10.1248/bpb.31.118
44. Gershanik T, Benita S. Self-dispersing lipid formulations for improving oral absorption of lipophilic drugs. *Eur J Pharm Biopharm*. 2000;50 (1):179–188. doi:10.1016/s0939-6411(00)00089-8
45. Cerpnjak K, Zvonar A, Gasperlin M, et al. Lipid-based systems as a promising approach for enhancing the bioavailability of poorly water-soluble drugs. *Acta Pharm*. 2013;63(4):427–445. doi:10.2478/acph-2013-0040
46. Pouton CW, Porter CJ. Formulation of lipid-based delivery systems for oral administration: materials, methods and strategies. *Adv Drug Deliv Rev*. 2008;60(6):625–637. doi:10.1016/j.addr.2007.10.010
47. Avachat AM, Patel VG. Self nanoemulsifying drug delivery system of stabilized ellagic acid-phospholipid complex with improved dissolution and permeability. *Saudi Pharm J*. 2015;23(3):276–289. doi:10.1016/j.jsps.2014.11.001
48. McConville C, Friend D. Development and characterisation of a self-microemulsifying drug delivery systems (SMEDDSs) for the vaginal administration of the antiretroviral UC-781. *Eur J Pharm Biopharm*. 2013;83(3):322–329. doi:10.1016/j.ejpb.2012.10.007
49. Elnaggar YS, El-Massik MA, Abdallah OY. Self-nanoemulsifying drug delivery systems of tamoxifen citrate: design and optimization. *Int J Pharm*. 2009;380(1–2):133–141. doi:10.1016/j.ijpharm.2009.07.015
50. Bandyopadhyay S, Katare OP, Singh B. Optimized self nano-emulsifying systems of ezetimibe with enhanced bioavailability potential using long chain and medium chain triglycerides. *Colloids Surf B Biointerfaces*. 2012;100:50–61. doi:10.1016/j.colsurfb.2012.05.019
51. Li F, Hu R, Wang B, et al. Self-microemulsifying drug delivery system for improving the bioavailability of huperzine A by lymphatic uptake. *Acta Pharm Sin B*. 2017;7(3):353–360. doi:10.1016/j.apsb.2017.02.002
52. Liao H, Gao Y, Lian C, et al. Oral absorption and lymphatic transport of baicalein following drug-phospholipid complex incorporation in self-microemulsifying drug delivery systems. *Int J Nanomed*. 2019;14:7291–7306. doi:10.2147/IJN.S214883
53. Qiao J, Ji D, Sun S, et al. Oral bioavailability and lymphatic transport of pueraria flavone-loaded self-emulsifying drug-delivery systems containing sodium taurocholate in rats. *Pharmaceutics*. 2018;10(3):147. doi:10.3390/pharmaceutics10030147
54. Kim DS, Cho JH, Park JH, et al. Self-microemulsifying drug delivery system (SMEDDS) for improved oral delivery and photostability of methotrexate. *Int J Nanomed*. 2019;14:4949–4960. doi:10.2147/IJN.S211014
55. Lee JH, Lee GW. Formulation approaches for improving the dissolution behavior and bioavailability of tolvaptan using SMEDDS. *Pharmaceutics*. 2022;14(2):415. doi:10.3390/pharmaceutics14020415
56. Verma R, Kaushik D. Design and optimization of candesartan loaded self-nanoemulsifying drug delivery system for improving its dissolution rate and pharmacodynamic potential. *Drug Deliv*. 2020;27(1):756–771. doi:10.1080/10717544.2020.1760961
57. Nardin I, Kollner S. Successful development of oral SEDDS: screening of excipients from the industrial point of view. *Adv Drug Deliv Rev*. 2019;142:128–140. doi:10.1016/j.addr.2018.10.014
58. Gurjar R, Chan CYS, Curley P, et al. Inhibitory effects of commonly used excipients on P-glycoprotein in vitro. *Mol Pharm*. 2018;15 (11):4835–4842. doi:10.1021/acs.molpharmaceut.8b00482
59. Das S, Lee SH, Chia VD, et al. Development of microemulsion based topical ivermectin formulations: pre-formulation and formulation studies. *Colloids Surf B Biointerfaces*. 2020;189:110823. doi:10.1016/j.colsurfb.2020.110823